



SEISMIC PERFORMANCE AND DESIGN OF AUTOCLAVED AERATED CONCRETE (AAC) STRUCTURAL SYSTEMS

Jennifer TANNER^{1,3}, Jorge VARELA^{2,3}, Matthew BRIGHTMAN³, Ulises CANCINO³, Jaime ARGUDO^{3,4}, and Richard KLINGNER⁵

SUMMARY

To facilitate the use of autoclaved aerated concrete (AAC) in the US, consensus design provisions have been proposed based on an integrated seismic-qualification program carried out at The University of Texas at Austin. That program focused on shear walls, the fundamental lateral force-resisting element of AAC structures.

The first phase of the experimental program consisted of tests on a suite of 17 shear wall specimens (10 shear-dominated and 7 flexure-dominated) subjected to quasi-static, reversed cyclic, in-plane lateral loading with applied axial load to simulate gravity loading. The results of these tests, combined with those of similar tests performed by other investigators, revealed predictable behavioral modes for both shear-dominated and flexure-dominated AAC shear walls. A two-story, full-scale AAC assemblage specimen was then designed and tested as the culmination of the testing program. The assemblage specimen contained two flanged AAC shear walls and two AAC diaphragms consisting of untopped AAC panels oriented perpendicular to the direction of load in the first elevated level and parallel to the direction of loading in the second elevated level. The results of this test verified that load can be successfully transferred from AAC diaphragms to AAC shear walls through typical AAC construction details. This assemblage specimen also verified that AAC structural systems behave according to the predictive models verified in the suite of 17 shear walls tested at UT Austin. Furthermore, the behavior of this AAC assemblage specimen illustrated that AAC shear walls, even with aspect ratios of about 1.0, can be designed to fail in flexure and to reach displacement ductilities between 2.5 and 6.

INTRODUCTION

Autoclaved Aerated Concrete (AAC), a lightweight cementitious material originally developed in Europe more than 70 years ago, has recently been introduced into the US. To facilitate the use of AAC in the US, consensus design provisions have been proposed based on an integrated seismic-qualification program that has been carried out at The University of Texas at Austin. That program considered shear walls, the fundamental lateral force-resisting element of AAC structures. The geometry, wall configuration and

¹ Assistant Professor in Civil Engineering, the University of Wyoming, Laramie, WY 82071

² Assistant Professor in Civil Engineering, Autonomous University of Yucatan, Yucatan, Mexico

³ Former Graduate Research Assistant, The University of Texas at Austin, Austin, TX 78712

⁴ Current Graduate Research Assistant, The University of Texas at Austin, Austin, TX 78712

⁵ L. P. Gilvin Professor in Civil Engineering, The University of Texas, Austin, TX 78712

axial load of each of 17 AAC shear-wall specimens tested at UT Austin are presented in Table 1. The objectives of the tests were to develop reliable design provisions for flexure- and shear-dominated AAC shear walls.

Table 1: Overview of AAC shear wall specimens tested at The University of Texas at Austin

Specimen (Manufacturer)	Length in. (m)	Height in. (m)	Thickness in. (m)	Axial Load kips (kN)	Exterior Reinforcement	Interior Reinforcement
1	240 (6.1)	154 (3.9)	8 (0.2)	156 (694)	2-B7 1 in. (25 mm) 24 in.(0.6 m) from ends	No
2	240 (6.1)	154 (3.9)	8 (0.2)	156 (694)	2-B7 1 in. (25 mm) 24 in.(0.6 m) from ends	No
3	240 (6.1)	152 (3.8)	8 (0.2)	120 (534)	2-B7 1 in. (25 mm) 24 in.(0.6 m) from ends	No
4	240 (6.1)	154 (3.9)	8 (0.2)	120 (534)	2-B7 1 in. (25 mm) 24 in.(0.6 m) from ends	#5 (16 mm) at 48 in. (1.2 m)
5	240 (6.1)	152 (3.8)	8 (0.2)	60 (267)	2-B7 1 in. (25 mm) 24 in.(0.6 m) from ends	No
7	144 (3.7)	152 (3.8)	8 (0.2)	80 (356)	2-B7 1 in. (25 mm) 24 in.(0.6 m) from ends	No
9	96 (2.4)	154 (3.9)	8 (0.2)	60 (267)	2-B7 1 in. (25 mm) right at wall ends	No
11	48 (1.2)	152 (3.8)	8 (0.2)	25 (111)	2-B7 1 in. (25 mm) right at wall ends	No
13	72 (2.1)	154 (3.9)	8 (0.2)	25 (111)	No	# 5 (16 mm) 12 in. (0.3 m) from ends
14a	56 (1.4)	154 (3.9)	10 (0.25)	5 (22)	No	# 5 (16 mm) 4 in. (0.1 m) from ends
14b	56 (1.4)	154 (3.9)	10 (0.25)	5 (22)	No	# 5 (16 mm) 4 in. (0.1 m) from ends
15a	112 (2.8)	154 (3.9)	10 (0.25)	25 (111)	No	# 5 (16 mm) 8 in. (0.2 m) from ends
15b	112 (2.8)	154 (3.9)	10 (0.25)	25 (111)	No	# 5 (16 mm) 8 in. (0.2 m) from ends
16	112 (2.8)	154 (3.9)	10 (0.25)	25 (111)	No	# 5 (16 mm) 8 in. (0.2 m) from ends
17	112 (2.8)	154 (3.9)	10 (0.25)	25 (111)	No	# 5 (16 mm) 4 in. (0.1 m) from ends
18	144 (3.7)	152 (3.8)	8 (0.2)	45 (200)	2-B7 1 in. (25 mm) 12 in.(0.3 m) from ends	# 5 (16 mm) 12 in. (0.3 m) from ends
19	216 (5.5)	152 (3.8)	8 (0.2)	58 (258)	2-B7 1 in. (25 mm) 24 in.(0.6 m) from ends	#5 (16 mm) at 48 in. (1.2 m)
Assemblage	Each wall 240 (6.1)	Both stories 200 (5.1)	10 (0.25)	Each wall 30 (133)	No	# 5 (16 mm) 24 in. (0.2 m) from ends

The culmination of the testing program was a Two-story Assemblage Specimen, tested to verify that a system of squat AAC shear walls designed to behave in flexure would indeed do so; to verify the proposed design provisions for AAC shear walls and floor diaphragms; to verify proposed analytical models for such elements and systems; and to verify proposed seismic design procedures for AAC structural systems.

The Two-Story AAC Assemblage Specimen consisted of two flanged walls connected by floor slabs, as shown in three-dimensional view in Figure 1. The walls were constructed with vertical AAC panels, and the floor slabs were constructed with untopped AAC floor panels. Vertical panels were selected for the assemblage because these are potentially the most vulnerable configuration, based on the observed behavior of single-story, lineal AAC shear walls. On the upper level, the floor panels were oriented longitudinally; in this configuration, design of lateral load transfer is based on dowel action of steel placed in grouted keys. On the lower level, the floor panels were oriented transversely; in this configuration design of lateral load transfer is based on adhesion or a truss mechanism (Tanner [8]).

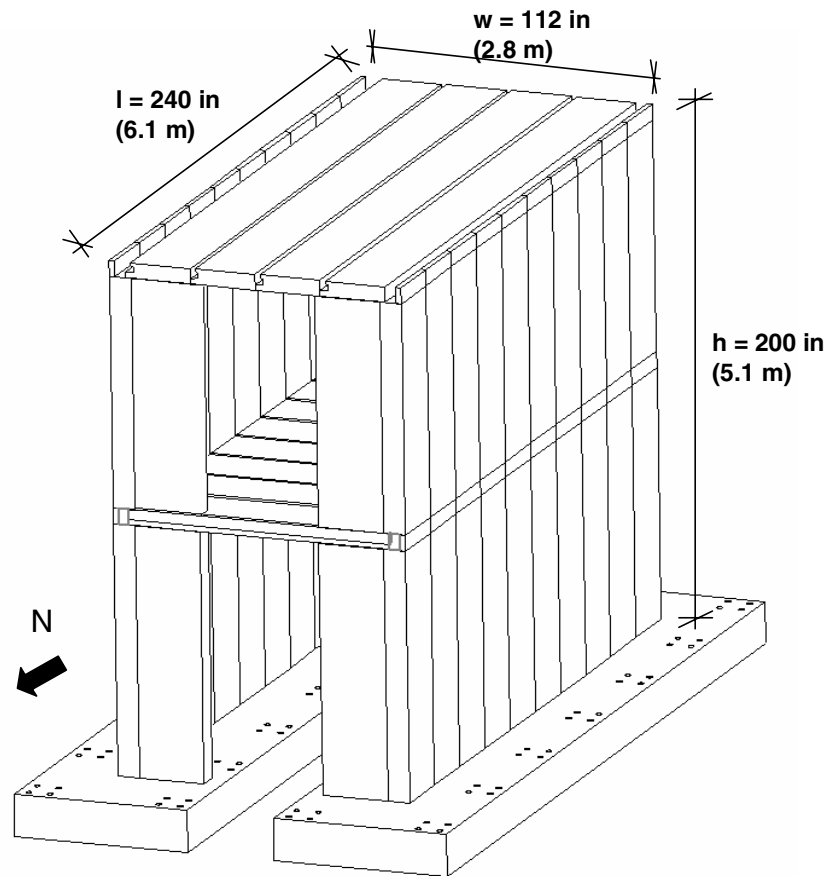


Figure 1: Three-dimensional view of Two-story AAC Assemblage Specimen

The plan dimensions of 20 ft (6.1 m) long by 9.33 ft (2.8 m) wide were governed by laboratory space restrictions. The wall length of 20 ft. (6.1 m) was selected in order to meet the design goal of flexural behavior in a squat wall. This was achieved by using minimal flexural reinforcement, placed only at the ends of the longest factory produced panel. Since vertical panels are manufactured with cores placed at head joints only, vertical reinforcement (four #4 bars (12 mm)), was placed in the vertical joints between the outside two panels at each end of each web. Additional dowels (three #4 (16 mm)) were placed at the base and at the first elevated floor slab to increase the design sliding-shear capacity of each wall.

In the following sections the test setup, test results of shear walls, test results of assemblage specimen and conclusions are presented.

TEST SETUP FOR SHEAR WALLS AND ASSEMBLAGE SPECIMEN

The AAC shear-wall specimens tested at The University of Texas at Austin were constructed on a concrete foundation post-tensioned to the strong floor at the Ferguson Structural Engineering Laboratory. Each shear wall was constructed on a leveling bed of masonry mortar placed on the concrete foundation. A very stiff longitudinally post-tensioned loading beam was placed on top of the specimen. Reversed cyclic lateral load was applied to each specimen using either one or two hydraulic rams mounted to a strong wall and supplied through a manually controlled hydraulic pump. The planned in-plane loading history for the shear wall specimens consisted of a series of reversed cycles to monotonically increasing maximum load. The test setup for a masonry-type wall is shown in Figure 2.

At UT Austin, axial load was applied through hydraulic rams, post-tensioned rods or a combination of the two. Net axial force was maintained approximately constant under reversed cyclic loading by using a mechanical “load maintainer” and by ensuring that some post-tensioning force remained in the external rods. A complete description of the test set-up and results is presented in Brightman [3], Tanner (2003) and Varela (2003). The test setup for AAC shear walls tested by Hebel AG (and used for comparison with results from UT Austin) was similar, except the axial load was not held constant throughout the test (Tanner [8]).

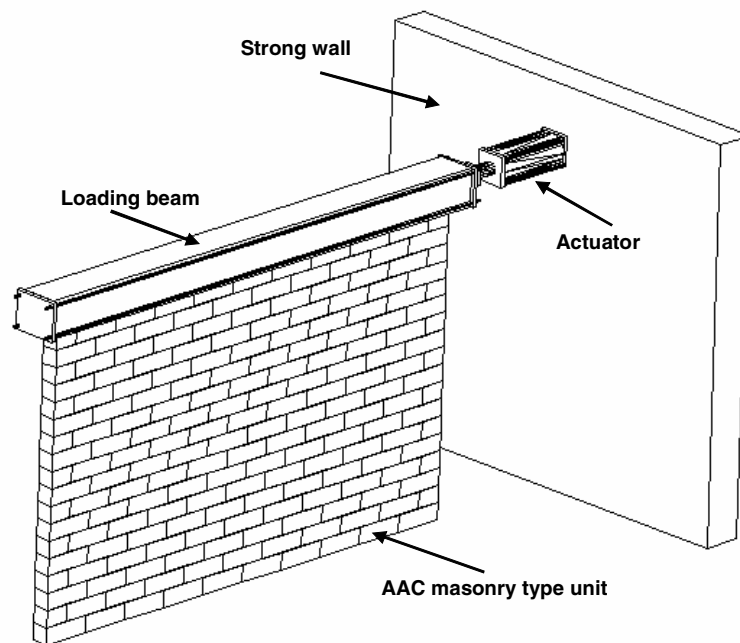


Figure 2: Test setup for shear walls tested at U.T. Austin

The geometry, flexural reinforcement, and axial force for each shear wall specimen were selected to induce either shear- or flexure-dominated behavior, as desired. The shear-dominated specimens were over-reinforced in flexure using external threaded rods as flexural reinforcement. In most specimens, these supplemental rods were also pre-tensioned to increase the axial load in the wall. The flexure-dominated specimens were lightly reinforced in flexure. The reinforcement in each specimen is summarized in Table 1 (Varela [10]; Tanner [8]).

The culmination of the research project was the Two-story Assemblage Specimen. The lateral load was applied to each floor slab through two concrete loading beams, one above and one below each floor slab, clamped together by vertical rods. The lateral load was applied through frictional resistance between the concrete loading beam and the floor slab. Equivalent lateral loads were applied at each floor slab. The procedure followed to determine the loading history was the same as for the shear wall specimens. Axial load on the assemblage specimen came from the weight of the floor slab plus the loading equipment. The total axial load at the base of each wall is 30.2 kips (133 kN). The respective loads on the first and second elevated slabs were 100 psf (4.8 kPa) and 160 psf (7.7 kPa). These equivalent loads on the prototype represent a heavily loaded floor slab which is a reasonable level of dead and live load. A detailed description of this test set-up and results is found in Tanner (2003) and Varela (2003).

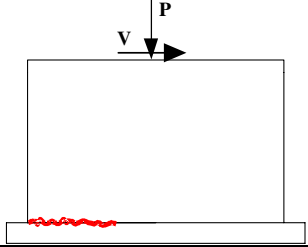
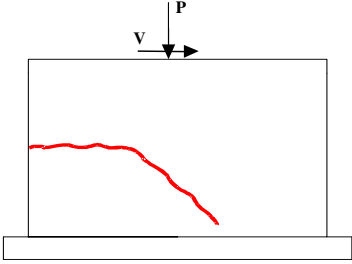
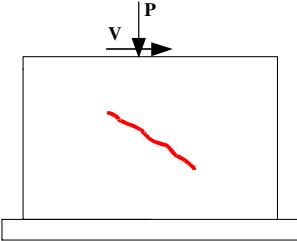
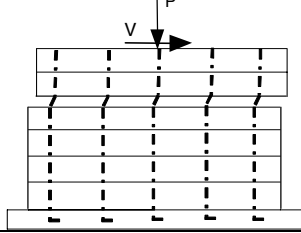
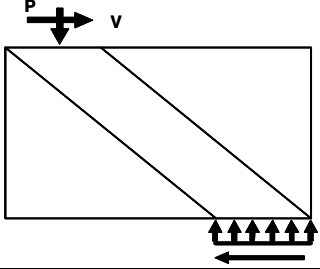
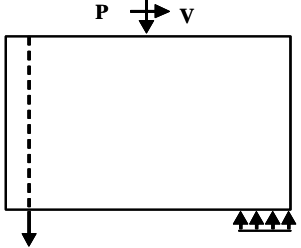
TEST RESULTS FOR SHEAR WALLS AND ASSEMBLAGE SPECIMEN

The following behavioral modes were observed in either the flexure-dominated or the shear-dominated wall specimens: flexural cracking; flexure-shear cracking; web-shear cracking; crushing of the diagonal strut; and nominal flexural capacity. An equation was proposed to predict the onset of each behavior in a shear wall specimen. A picture of an arbitrary wall subject to each behavior and the resulting predictive equation is presented in Table 2. A brief justification of the proposed equations is presented in the following paragraphs followed by a discussion of the observed hysteretic behavior of the specimens.

Flexural cracking

In flexural cracking of AAC shear walls, a flexural crack forms at the base of the tensile side of the wall, between the AAC and the leveling bed. Flexural cracking is governed by the modulus of rupture of the AAC, or by the tensile bond between the AAC material and the leveling bed if such a joint is present in the shear wall under consideration. Flexural cracking was observed in 15 shear-wall specimens tested at UT Austin. In all cases, these flexural cracks formed between the AAC and the masonry leveling bed. The observed smooth failure surface indicates tensile bond failure rather than an AAC material failure. Using the lateral loads at which flexural cracking was observed, tensile bond strengths were back-calculated for each shear wall. These results are presented in Table 2. The mean modulus of rupture is 70.5 psi (0.46 MPa), and the corresponding 20% fractile is 53 psi (0.34 MPa). The proposed design value for modulus of rupture should not exceed 50 psi (0.34 MPa) if a leveling bed joint is present in the AAC element (Tanner [8]; Cancino 2003).

Table 2: Description and prediction of each major event

Prediction of behavior	Description of behavior
<p>Flexural cracking</p> $V_{cr} = \frac{S}{h} \left(f_{rAAC} + \frac{P}{l_w t} \right)$ <p>f_r is minimum of modulus of rupture of AAC or tensile bond strength of the material and AAC</p>	
<p>Flexure-shear cracking</p> $V_{AAC} = \frac{S \cdot \left(f_{bond} + \frac{P}{l_w t} \right)}{\left(\frac{M}{V} - \frac{l_w}{2} \right)}$ <p>$f_{bond} = 0.04 f_{AAC} + 66$ valid for $f_{AAC} > 450$ psi</p>	
<p>Web-shear cracking</p> $V_{AAC} = 0.9 l_w t \sqrt{f'_{AAC}} \sqrt{1 + \frac{P_u}{2.4 \sqrt{f'_{AAC}} l_w t}}$ <p>f_{AAC}' in psi, P_u in lbs, l_w and t in in.</p>	
<p>Sliding shear</p> $V_{ss} = \mu P_u$	
<p>Crushing of diagonal strut</p> $V_{ds} = 0.9 \cdot f_{AAC}' \cdot t \cdot w_{strut} \left[\frac{h \cdot \left(\frac{3}{4} l_w \right)}{h^2 + \left(\frac{3}{4} l_w \right)^2} \right]$	
<p>Nominal flexural capacity</p> <p>Equation for an individual wall is based on traditional flexural theory for the wall's geometry, reinforcement and axial load.</p>	

Flexure-shear cracking

A flexure-shear crack begins as a horizontal crack at a height of about one-half the plan length of the wall (l_w) above the base of the wall, and then propagates diagonally through the center of the wall. In the equation for flexural cracking the term h is replaced by $(M/V-l_w/2)$ which represents the height at the location of the flexural portion of the crack (at an assumed height of $l_w/2$). Flexure-shear cracking was observed in the seven flexure-dominated shear-wall specimens. In every case the flexural portion of the flexure-shear crack formed first in the horizontal joint (Tanner [8]; Cancino 2003), indicating that this joint is weaker than the AAC material itself. Relationships for the tensile bond strength, f_{bond} , between AAC and thin-bed mortar as a function of density and compressive strength were determined by Argudo [1].

The ratios of observed to predicted flexure-shear cracking capacities of the AAC shear walls were calculated for each specimen. The true height of the flexural portion of the flexure-shear crack was substituted for the assumed value of $l_w/2$ in the denominator of the equation for flexure-shear cracking. Where the tensile bond strength between AAC and thin-bed mortar was lower than the modulus of rupture, the equations proposed by Argudo [1] were used. Based on the relationship between compressive strength and bond strength, with the exception of Shear Wall Specimen 14a, the ratios of observed to predicted strength range from 1.0 to 1.4 with a mean of 1.18 and a COV of 8.9%. Based on the relationship between density and bond strength the mean ratio of observed to predicted strength is 1.15 with a COV of 6.5% (Tanner [8]). Although the formation of flexure-shear cracks can be predicted, no code language is proposed for flexure-shear cracking, because that formation was not accompanied by a decrease in strength or stiffness of the specimens (Tanner [8]). Furthermore, vertical reinforcement was sufficient to resist the moment at the base of the wall after flexure-shear cracking, thus maintaining the shear capacity.

Web-shear cracking

Web-shear cracks formed in the shear-dominated specimens tested at UT Austin and in tests performed by Hebel AG in Germany⁶ (Tanner [8]). Development of a design equation for capacity as governed by web-shear cracking began with development of an equation to determine the base shear when the maximum principal tensile stresses reach the splitting tensile strength of the material (Tanner [8]). The lateral loads at which web-shear cracking was observed and predicted were compared and a mean ratio of observed to predicted strength of 0.72 was determined with a corresponding COV of 13.8%. The ratios of observed to predicted behavior are plotted in Figure 3. The mean ratio of observed to predicted web-shear cracking capacity is plotted along with the lower 10% fractile of 0.59. These results show lower ratios of observed to predicted strengths, indicating that the initial prediction was unconservative. That equation was modified so that it would correspond to the 10% lower fractile of the ratios of observed to predicted capacities. This lower fractile is selected based on the low COV of test results and the number of specimens. The final equation to predict the web-shear cracking capacity of a shear-wall specimen is shown in Table 1.

⁶ Personal communication, Violandi Vratsanou, Hebel AG, Germany, November 2000.

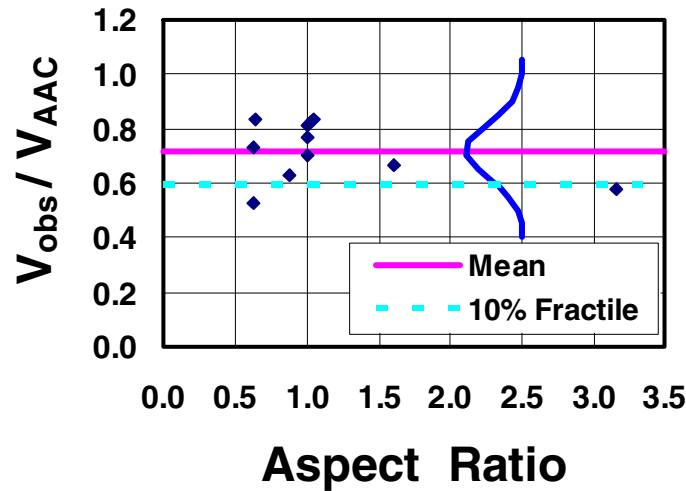


Figure 3: Observed versus predicted capacities as governed by web-shear cracking for specimens with fully mortared head joints

A similar evaluation was performed for a suite of nine AAC shear-wall specimens tested by Hebel AG, and consisting of modular blocks with the head joints left unmortared. The mean ratio of observed to predicted strength for this data is 0.46 with a COV of 13.1%. The corresponding 10% lower fractile is 0.38. Based on the methodology presented above a separate equation was created for shear-wall specimens with modular blocks whose head joints are unmortared (Tanner [8]).

Contribution of shear reinforcement

In conventional reinforced concrete design, the contribution of shear reinforcement, V_s , is included by adding it directly to the nominal shear cracking capacity of the concrete. The proposed design provisions for AAC shear walls permit the inclusion of the V_s contribution, but only from deformed horizontal reinforcement embedded in grout. They conservatively neglect the contribution of all other horizontal reinforcement embedded in AAC, based on the observed behavior of lintels tested at The University of Western Australia and shear-wall specimens tested at UT Austin (Boutros and Saverimutto [2]; Tanner [8]).

The capacity of shear reinforcement embedded in AAC may be limited by bearing of steel perpendicular to the shear reinforcement on surrounding AAC. Under reversed cyclic loads, the contribution to shear reinforcement may be further limited by progressive crushing of the AAC under the reinforcement perpendicular to the shear reinforcement. When the AAC ahead of the perpendicular reinforcement or cross wires crushes, a void forms behind the cross wires (Figure 4). Under reversed cyclic loading voids form ahead of and behind the cross wires or perpendicular reinforcement (Figure 5). Until sufficient displacement is reached to move through this void and again bear on the AAC, the shear resistance due to shear reinforcement is negligible. Primarily for this reason the contribution of shear reinforcement from factory-placed welded wire fabric is conservatively neglected.

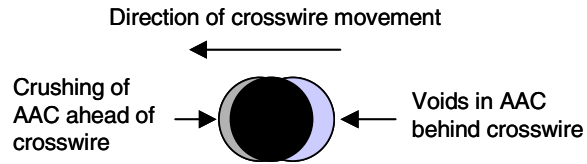


Figure 4: Voids caused by the crushing of AAC under monotonic loading

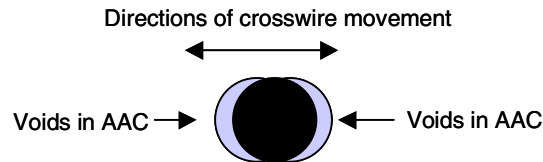


Figure 5: Voids caused by the crushing of AAC under cyclic loading

Sliding shear capacity

An AAC shear wall of horizontal panels or masonry-type blocks exhibits a bed-joint crack when the shear stress on the bed joints exceeds the interface shear capacity, v . Sliding shear capacity is the product of the coefficient of friction across the potential failure interface, and the force acting normal to that interface. This mechanism, commonly referred to as “shear friction,” includes normal forces from reinforcement crossing the interface, and from externally applied load normal to it. In traditional shear friction, sliding over a rough joint causes widening of the crack, stressing the vertical reinforcement crossing the crack and creating additional clamping force. Under reversed cyclic loading of AAC, this resistance can degrade so that resistance to sliding shear is provided primarily by dowel action of reinforcement crossing the bed joints. This contribution to V_{ss} is limited by the product of the area of the reinforcement perpendicular to the potential failure interface and the yield strength of that reinforcement in shear, about $0.6f_y$. This contribution to sliding shear capacity shown is augmented by some capacity due to friction.

Sliding shear was observed in Shear Wall Specimen 4 and the Two-story Assemblage Specimen. In these specimens the initial sliding shear capacity approximated the contribution of frictional resistance and dowel action combined. As damage in the wall increased the effectiveness of the dowel action was reduced. This observed decrease in dowel action is based on the loss of material surrounding the dowel. Detailed verification of this observed strength decrease is presented in Tanner [8]. The prediction for sliding shear capacity is conservatively taken as the component due to friction alone.

Crushing of the diagonal strut

As axial load increases, the shear capacity of an AAC shear wall as governed by web-shear cracking also increases. If these axial loads are accompanied by significant shear, as in a low-rise wall, the wall's shear capacity may be limited by crushing along the compression diagonal. Diagonal crushing can be predicted using a strut-and-tie model consisting of two elements: a diagonal compression strut (F_{strut}); and a tension tie-down force (T). The compressive force in the diagonal strut is the resultant of the vertical tie-down forces and the applied horizontal load. Because the system is statically determinate, the vertical component is the summation of the force in the tie-down rods, and the horizontal component is the applied lateral load (V).

The compressive force transferred along the diagonal strut is equilibrated at the base of the wall by the frictional resistance (acting horizontally) and the vertical component of compression in the diagonal strut. The proposed design provisions and justification for capacity equations for this limit state are presented in the following paragraphs.

The geometry of a shear-wall specimen with aspect ratio of 0.6 and horizontal projection of the strut (l_{strut}) equal to one-quarter of the plan length of the wall, is shown in the left side of Figure 6. From geometry, the force in the strut will be 1.7 times the vertical reaction (ratio of diagonal leg to vertical leg of equivalent triangle). For a squat wall, the diagonal strut can crush at lateral loads smaller than those corresponding to the wall's nominal flexural capacity. Because of the inclination of the strut, the force in the compression diagonal of a squat wall can be much higher than the flexural compression in the wall toe.

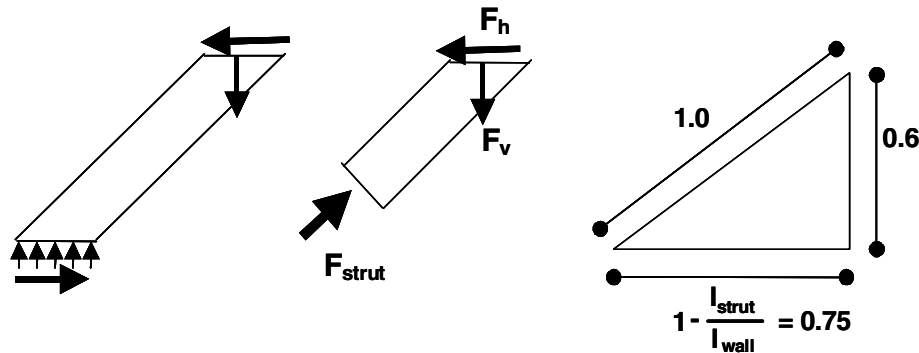


Figure 6: Relationship of forces in the diagonal strut

Crushing of the diagonal strut was observed in Shear Wall Specimen 1. The length of crushing extended one quarter of the plan length of the wall. Based on the applied load at crushing and the geometry of the wall, the proposed equation for crushing of the diagonal strut was calibrated. It represents the horizontal force (V) at crushing based on equilibrium of horizontal forces at the base of the diagonal strut. The derivation for this equation is developed in Tanner (2003). In the remaining shear-wall specimens crushing of the diagonal strut was avoided by limiting the axial load. The validity of the proposed equation was indirectly determined by the fact that crushing of the diagonal strut was not observed in subsequent specimens. Although this equation is far from perfect, it was a reliable tool for avoiding crushing of the diagonal strut in the AAC shear walls tested in this study.

Nominal flexural capacity

The nominal flexural capacity of AAC shear walls can be determined based on equilibrium of a cross-section. General assumptions for flexural behavior were verified in the flexure-dominated shear-wall specimens. The compressive zone is determined based on a linear strain relationship, using a maximum useful compressive strain in the AAC of 0.003 (Argudo [1]), and an equivalent rectangular stress block whose height is $0.85f_{AAC}'$ (or $0.85f_m'$), and whose depth is β_1c , where $\beta_1 = 0.67$. The value of β_1 is selected to maintain equilibrium between the equivalent stress block and a triangular compressive stress distribution based on tested stress-strain results of Argudo [1].

Observed versus predicted nominal flexural capacities can be compared for flexure-dominated Shear Wall Specimen 14a, 14b, 15a, 15b and 17. The nominal flexural capacity for these specimens was calculated using a steel yield strength of 75 ksi (490 MPa), based on mill reports. The ratios of observed to predicted strength range from 1.11 to 1.34, with an average of 1.22 and a COV of 6.8%. A refined analysis was performed considering strain hardening using RCCOLA [6]. With this refinement the range of observed to predicted nominal flexural capacity ranges from 0.95 to 1.15. The average is 1.06 with a COV of 7.0%. The extent of strain hardening in the flexural reinforcement is based on the steel strain, which depends on the longitudinal deformation at the tensile reinforcement divided by the unbonded length of that reinforcement. The unbonded length decreases as the bar size decreases, and can result in yielding and strain-hardening of small-diameter bars even at low drift levels.

Hysteretic behavior of specimens

The observed displacement ductilities (final displacement divided by the displacement at yielding of the flexural reinforcement) of the flexure-dominated shear wall specimens ranged from 4.8 to 6.9 while loading to the south and from 1.7 to 5.8 while loading to the north. The low displacement ductility of 1.7 while loading to the north was observed in Shear Wall Specimen 16 and is attributed to early damage to the compression toe and a spurious increase in axial load during this test. If this data point is removed, the observed displacement ductilities range from 2.6 to 6.0 with an average of 4.8 (Varela [10]). The observed drift in the flexure-dominated specimens during stable cycles ranged from 0.4 to 1.9. As with displacement ductility the low value of drift occurred while loading to the north of Shear Wall Specimen 16. If this value is removed the drift ratios obtained range from 1.0 to 1.9 with an average of 1.2 (Varela [10]). The displacement ductilities and drift ratios of the shear-dominated specimens were lower. This is expected since the shear-dominated walls are designed to behave in the elastic range. A complete description of the hysteretic behavior of each specimen is presented in Varela [10].

The hysteretic behavior of the Two-story Assemblage Specimen is presented Figure 7. The force-displacement behavior is initially linear elastic. Stable flexural hysteretic loops are presented with a decrease in peak load less than 10% of the previous cycle until the final cycle, despite the unexpected presence of web-shear cracks, which formed because the AAC material was of lower strength than that anticipated in design (Varela [10], Tanner [8]). Hysteretic behavior would have improved had those web-shear cracks not formed.

The effect of sliding in the Two-story Assemblage Specimen can be removed to evaluate the ductility and flexural performance of the assemblage specimen as shown in Figure 8. After removing the base slip, the individual shear walls reached drift ratios between 0.24% and 0.42%, with final displacement ductilities ranging from 2.5 to 6. The correction for slip in the final cycle of the east wall includes an assumption for the slip. If this cycle were eliminated the displacement ductility would decrease to 5.3, a 10% difference.

Including base slip, the Two-story Assemblage Specimen reached drift ratios between 0.7% and 0.8%. Final displacement ductilities ranged from 7.8 to 12 (Tanner [8], Varela [10]).

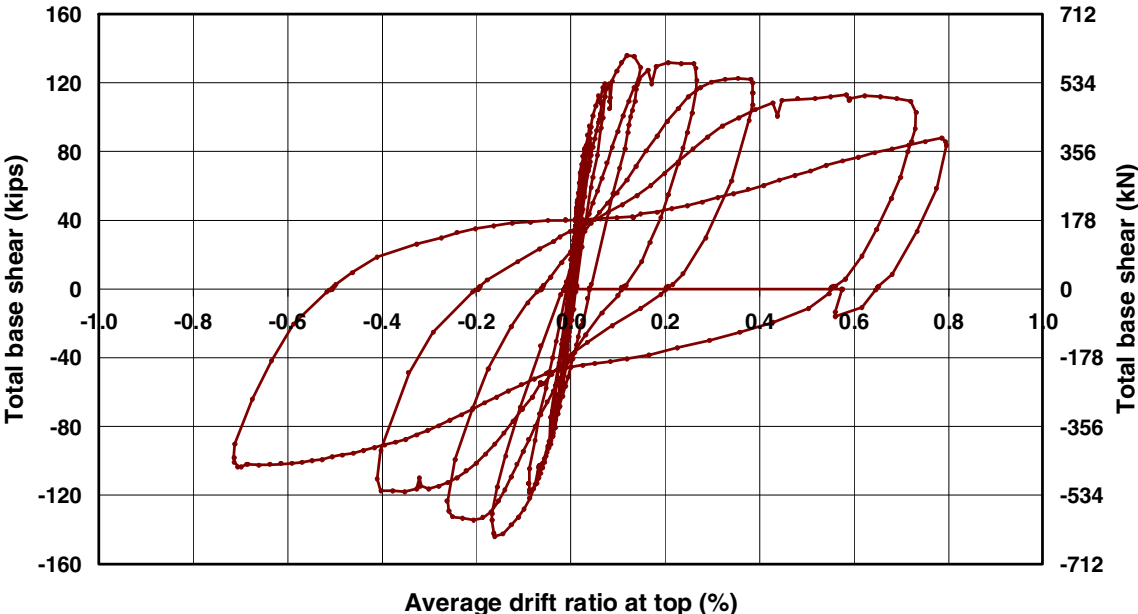


Figure 7: Overall hysteretic behavior of Two-story Assemblage Specimen

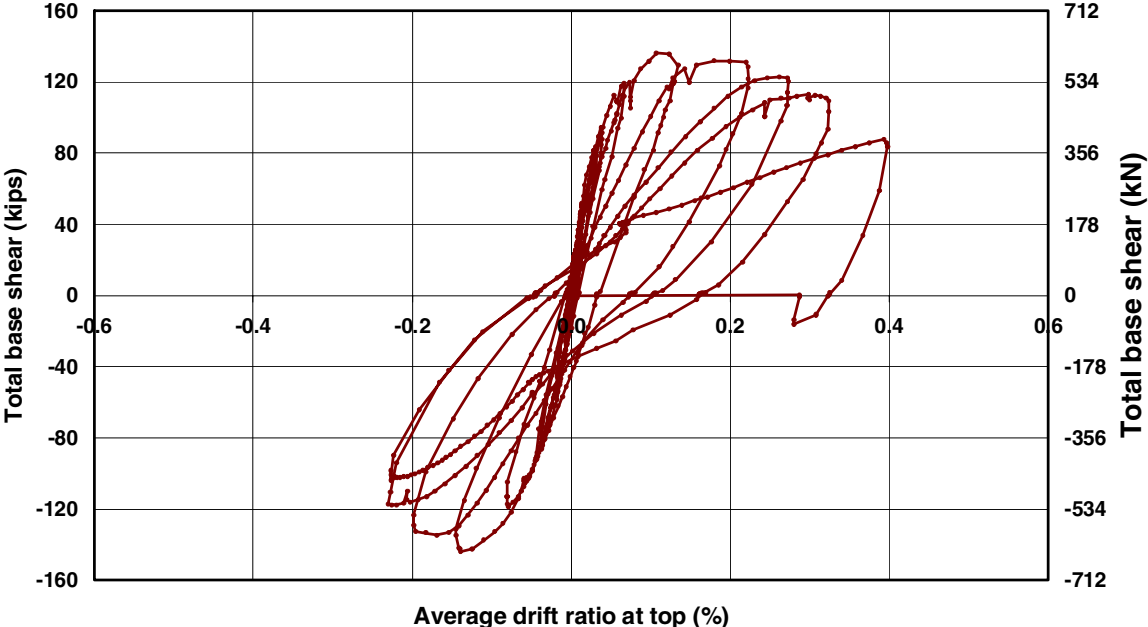


Figure 8: Hysteretic behavior of Two-story Assemblage Specimen with slip removed

CONCLUSIONS

Based on test results from The University of Texas at Austin and elsewhere, procedures and corresponding provisions have been proposed for the design of AAC shear walls made of masonry-type units or horizontally oriented reinforced panels. The proposed design procedures address flexural cracking, flexure-shear cracking, web-shear cracking, sliding shear, crushing of the diagonal strut and nominal flexural capacity. The proposed provisions are reliable, with low coefficients of variation (generally below 15%) and values close to or exceeding 1.0 for the ratios of observed capacity to the capacity predicted using equations based on the tested strength.

The Two-Story AAC Assemblage Specimen met its required objectives. The shear walls conformed to the predictive models for flexural cracking and web-shear cracking. Damage did not occur in the AAC floor slabs or their connections to the walls, verifying that the proposed design provisions based on adhesion would produce a structure whose behavior was governed by the behavior of the shear walls.

Although the Two-story Assemblage Specimen exhibited web-shear cracking, stable hysteretic loops were achieved. With the effects of sliding removed, drift levels exceeded 0.3%, and displacement ductilities ranged from 2.5 to 6. For design purposes, these results justify the assumption of an available displacement ductility of at least 2.5. Based on previous tests of flexure-dominated AAC shear walls at UT Austin, this ductility would have been increased if the anomalous web-shear cracking had not occurred (Varela [10]). This test confirms that the design objective of flexure-dominated behavior can be achieved even in relatively squat walls.

ACKNOWLEDGEMENTS

The information reported here is based on a research project on the Seismic Behavior of Autoclaved Aerated Concrete, conducted at The University of Texas at Austin, under the sponsorship of the Autoclaved Aerated Concrete Products Association. The authors also wish to express their gratitude to the staff and students at the Ferguson Structural Engineering Laboratory who assisted in the testing process, in particular Geoff Mitchell and Ross Sassen.

REFERENCES

1. Argudo, J.F., "Evaluation and Synthesis of Experiential Data for Autoclaved Aerated Concrete," *MS Thesis*, Department of Civil Engineering at The University of Texas at Austin, August 2003.
2. Boutros, M. and Saverimutto, L., "Anchorage Capacity of Reinforcing Bars in Autoclaved Aerated Concrete Lintels," *Materials and Structures*, November 1997.
3. Brightman, M., "AAC Shear Wall Specimens: Development of Test Setup and Preliminary Results," *MS Thesis*, Department of Civil Engineering at The University of Texas at Austin, May 2000.
4. Cancino, U., "Shear Wall Specimens of Low Strength AAC," *MS Thesis*, Department of Civil Engineering at The University of Texas at Austin, December 2003.
5. Klingner, R.E., Tanner, J.E., Varela J.L., Brightman, M.J., Argudo, J.F. and Cancino, U.L., "Technical Justification for Proposed Design Provisions for AAC Structures: Introduction and

- Shear Wall Tests,” *ACI523A Special Publication*, ACI Fall Meeting, Boston, Massachusetts, 2003.
6. RCCOLA 1977: “RCCOLA, A Computer Program for Reinforced Concrete Column Analysis, User's Manual and Documentation,” NISEE Software Library. University of California, Berkeley, CA.
 7. Tanner, J.E., Varela, J.L. and Klingner, R.E., “Seismic Testing of AAC Masonry Shear Walls” *Proceedings of the Ninth North American Masonry Conference*, Clemson, South Carolina, 2003, The Masonry Society.
 8. Tanner, J.E., “Design Provisions for AAC Structural Systems,” *PhD Dissertation*, Department of Civil Engineering at The University of Texas at Austin, May 2003.
 9. Varela, J.L., Tanner, J.E. and Klingner, R.E., “Development of R and C_D Factors for Seismic Design of AAC Structures,” *Proceedings of the Ninth North American Masonry Conference*, Clemson, South Carolina, 2003, The Masonry Society.
 10. Varela, J.L., “Development of R and C_D Factors for the Seismic Design of AAC Structures,” *PhD Dissertation*, Department of Civil Engineering at The University of Texas at Austin, May 2003.

NOTATION

f_{AAC}' = specified compressive strength of AAC
 f_{bond} = tensile bond strength of AAC
 f_{rAAC} = modulus of rupture of AAC
 h = height of shear wall
 l_w = plan length of shear wall
 M = acting moment at a given height of shear wall
 n_{cross} = number of layers of cross wires (vertical) between the failure surface and the closest panel end
 P = axial force acting on wall
 S = section modulus
 t = nominal thickness of shear wall
 V = acting shear at the base of shear wall
 V_{cr} = base shear at flexural cracking capacity
 V_{ds} = capacity of an AAC shear wall as governed by crushing of diagonal strut
 V_{AAC} = shear strength provided by AAC
 V_{ss} = sliding shear capacity of AAC shear wall
 W_{strut} = horizontal projection of the width of the diagonal strut
 μ = coefficient of friction